J. Fluid Mech. (1983), *vol.* 129, *pp.* 153–171
Printed in Great Britain

Nonlinear convection in a porous layer with finite conducting boundaries

By N. RIAHI
Department of Theoretical and Applied Mechanics, University of Illinois at Urbana–Champaign, Illinois 61801

(Received 7 October 1981 and in revised form 22 June 1982)

The problem of finite-amplitude thermal convection in a porous layer with finite conducting boundaries is investigated. The nonlinear problem of three-dimensional convection is solved by expanding the dependent variables in terms of powers of the amplitude of convection. The preferred mode of convection is determined by a stability analysis in which arbitrary infinitesimal disturbances are superimposed on the steady solutions. Square-flow-pattern convection is found to be preferred in a bounded region Γ in the (γ_b, γ_t)-space, where γ_b and γ_t are the ratios of the thermal conductivities of the lower and upper boundaries to that of the fluid. Two-dimensional rolls are found to be the preferred pattern outside Γ. The qualitative features of the convection problem appear to be essentially symmetric with respect to γ_b and γ_t. The dependence of the heat transported by convection on γ_b and γ_t is computed for the various solutions analysed in the paper.

1. Introduction

The present paper studies the problem of nonlinear thermal convection at small amplitude in a horizontal porous layer with finite conducting boundaries.

The problem of thermal convection in a porous medium is simpler than the corresponding one in an ordinary medium, since the equations of motion describing convection in a porous layer are of lower order than those describing Bénard convection. The qualitative features of thermal convection in a porous medium are, however, the same as those in an ordinary medium. Hence the problem of thermal convection in a porous medium is mathematically a simple one, which conveniently can be used to study nonlinear effects such as the preferred flow pattern.

The linear stability for the onset of convective flow in a porous medium was first investigated theoretically by Lapwood (1948). The subsequent nonlinear investigations of the problem such as those by Palm, Weber & Kvernvold (1972) and Straus (1974) are based on the assumption that the upper and lower boundaries have infinite thermal conductivity. Although this assumption is often well approximated in laboratory experiments, many convection problems in engineering and geophysics do not exhibit well-conducting boundaries, and the ratios γ_b and γ_t between the thermal conductivities of the lower and upper boundaries and that of the fluid must be taken into account as additional parameters.

The importance of the influence of the parameters γ_b and γ_t on small-amplitude nonlinear Bénard convection was first demonstrated by Busse & Riahi (1980, henceforth referred to as BR), who considered the case where γ_b and γ_t are equal ($\gamma_b = \gamma_t \equiv \gamma$) and assumed that the boundaries are nearly insulating ($\gamma \ll 1$). They found that the critical wavelength of the horizontal motion is proportional to $\gamma^{-\frac{1}{4}}$ and that square-pattern convection is preferred in contrast with two-dimensional rolls that represent the only form of stable convection in a symmetric layer with isothermal boundaries.

The goal of the analysis of the present paper is to isolate the nonlinear properties of thermal convection for arbitrary values of the parameters γ_b and γ_t. An important result of the present study is that there exist a bounded region Γ in (γ_b, γ_t)-space such that the preferred convection pattern is that of squares for $(\gamma_b, \gamma_t) \in \Gamma$. The preferred flow pattern is, however, two-dimensional rolls for $(\gamma_b, \gamma_t) \notin \Gamma$. This result demonstrates the enormous influence of the thermal boundary conditions on the preferred flow pattern.

The additional and interesting effect of the lateral boundaries in a finite system containing fluid-saturated porous material that have recently been studied for isothermal upper and lower boundaries (Zebib & Kassoy 1978; Straus & Schubert 1978, 1979, 1981; Schubert & Straus 1979) is expected to have significant influence on the realized flow pattern. This effect, however, is not considered here, since we are interested, in the present investigation, in studying the already complicated problem of the effect of arbitrary thermal-conducting upper and lower boundaries on nonlinear processes. We therefore assume that the fluid layer is infinitely long in the horizontal direction, which is appropriate for various applications in cases where the horizontal length of the layer is large compared to its thickness. This assumption enables us to understand the actual nonlinear properties and the convective motions that are not influenced by the lateral boundaries, and provides the foundation on which more detailed models can be built.

Sections 2–4 deal with the mathematical formulation of the problem, and the general description of steady convection and stability analysis. The steady solutions are discussed for various cases in §5, which is followed by some general discussion.

2. Mathematical formulation

We consider an infinite horizontal porous layer of depth d filled with fluid and heated from below. The layer is bounded above and below by two half-spaces with thermal conductivities λ_t^e and λ_b^e respectively. In the steady static state, a constant heat flux traverses the system such that temperatures T_1 and T_2 are attained at the upper and lower boundaries of the fluid. It is convenient to use non-dimensional variables in which lengths, velocities, time and temperature are scaled respectively by d, $\lambda/d\rho_0 c$, $d^2\rho_0 c/\lambda$ and $(T_2-T_1)R^{-1}$. Here λ is the thermal conductivity of the porous medium (fluid–solid mixture), ρ_0 is the reference density of the fluid, c is the specific heat at constant pressure and R is the Rayleigh number (defined below). Then, with the usual Boussinesq approximation that density variations are taken into account only in the buoyancy term, the Darcy–Boussinesq equations are

$$B\left(\frac{\partial \mathbf{u}}{\partial t}+\mathbf{u}\,.\,\nabla\mathbf{u}\right) = -\nabla p+\theta\mathbf{z}-\mathbf{u}, \tag{2.1a}$$

$$\nabla\,.\,\mathbf{u} = 0, \tag{2.1b}$$

$$\frac{\partial\theta}{\partial t}+\mathbf{u}\,.\,\nabla\theta = R\mathbf{u}\,.\,\mathbf{z}+\nabla^2\theta. \tag{2.1c}$$

Here $\mathbf{u}$ is the velocity vector, p is the modified deviation of pressure from its static value, θ is the deviation of temperature from its static value, $\mathbf{z}$ is a unit vector in the vertical direction, $B^{-1} = \nu d^2\rho_0 c/\lambda K$ is the so-called Prandtl–Darcy number and

$R = \beta g K(T_2 - T_1)\, d\rho_0 c/\nu\lambda$ is the Rayleigh number, with β the coefficient of thermal expansion, ν the kinematic viscosity, K the Darcy permeability coefficient and g the acceleration due to gravity.

The velocity vector $\mathbf{u}$ in (2.1) is defined according to Darcy's law as an average over the microscale of the porous medium. We shall assume that the microscale is small enough compared with any scale size of the flow for $\mathbf{u}$ to remain a well-defined quantity.

It is convenient to introduce a Cartesian system of coordinates, with the origin on the centreplane of the layer and with the z-coordinate in the vertical direction. The boundary conditions for θ and $\mathbf{u}$ are

$$\mathbf{u}\,.\,\mathbf{z} = 0 \quad \text{at} \quad z = \pm\tfrac{1}{2}, \tag{2.2a}$$

$$\frac{\partial \theta}{\partial z} = \gamma_{\mathrm{b}} \frac{\partial \theta_{\mathrm{b}}^{\mathrm{e}}}{\partial z}, \quad \theta = \theta_{\mathrm{b}}^{\mathrm{e}} \quad \text{at} \quad z = -\tfrac{1}{2}, \tag{2.2b}$$

$$\frac{\partial \theta}{\partial z} = \gamma_{\mathrm{t}} \frac{\partial \theta_{\mathrm{t}}^{\mathrm{e}}}{\partial z}, \quad \theta = \theta_{\mathrm{t}}^{\mathrm{e}} \quad \text{at} \quad z = \tfrac{1}{2}, \tag{2.2c}$$

where $\gamma_{\mathrm{b}} = \lambda_{\mathrm{b}}^{\mathrm{e}}/\lambda$, $\gamma_{\mathrm{t}} = \lambda_{\mathrm{t}}^{\mathrm{e}}/\lambda$, and $\theta_{\mathrm{b}}^{\mathrm{e}}$ and $\theta_{\mathrm{b}}^{\mathrm{t}}$ describe the deviation from the static temperature distribution in the spaces $z \leqslant -\frac{1}{2}$ and $z \geqslant \frac{1}{2}$ respectively. Since we have used the Darcy constitutive assumption in order to replace $\nabla^2\mathbf{u}$ with $-\mathbf{u}$ in (2.1), we cannot impose boundary conditions on the tangential components of $\mathbf{u}$. Equations (2.2) correspond to finite conducting boundaries through which no flow occurs.

We shall restrict our attention to the case of infinite Prandtl–Darcy number, in which case the left-hand side of (2.1a) vanishes. The physically appropriate value $B = 0$ follows from extraordinary small values of the permeability coefficient K in porous material: in sand $K = O(10^{-8})\ \mathrm{cm}^2$; in very porous fibre metals $K = O(10^{-4})\ \mathrm{cm}^2$.

The governing equations (2.1) can be simplified by using the general representation

$$\mathbf{u} = \boldsymbol{\delta}\Phi + \boldsymbol{\varepsilon}\psi, \tag{2.3a}$$

$$\boldsymbol{\delta} = \nabla \times \nabla \times \mathbf{z}, \quad \boldsymbol{\varepsilon} = \nabla \times \mathbf{z} \tag{2.3b}$$

for the divergence free velocity vector field $\mathbf{u}$. By taking the vertical component of the curl of (2.1a) it can be shown that the toroidal part $\nabla \times \mathbf{z}\psi$ of $\mathbf{u}$ must vanish for $B = 0$. Taking the vertical component of the curl of the curl of (2.1a) and using (2.3) in (2.1c) yields the following equations:

$$\Delta_2(\nabla^2\Phi + \theta) = 0, \tag{2.4a}$$

$$\nabla^2\theta - R\Delta_2\Phi = \boldsymbol{\delta}\Phi\,.\,\nabla\theta + \frac{\partial \theta}{\partial t}, \tag{2.4b}$$

where
$$\Delta_2 = \frac{\partial^2}{\partial x^2} + \frac{\partial^2}{\partial y^2}.$$

Equations (2.4) must then be solved subject to the boundary conditions (2.2b), (2.2c) and

$$\Phi = 0 \quad \text{at} \quad z = \pm\tfrac{1}{2}. \tag{2.5}$$

In the following sections we obtain the solutions by using the method of Schluter, Lortz & Busse (1965), treating the amplitude ϵ of convection as a small parameter.

3. Finite-amplitude steady convection

Using the energy method (Joseph 1976), it can be shown easily that small-amplitude steady solutions yield the lowest Rayleigh number R for which non-decaying solutions exist for the governing equations and the boundary conditions derived in §2. It is therefore appropriate for our small-amplitude convection analysis to consider the following expansions for θ, Φ and R in powers of ϵ:

$$\left.\begin{aligned}\begin{pmatrix}\theta\\ \Phi\end{pmatrix} &= \epsilon\begin{pmatrix}\theta_1\\ \Phi_1\end{pmatrix}+\epsilon^2\begin{pmatrix}\theta_2\\ \Phi_2\end{pmatrix}+\dots,\\ R &= R_0+\epsilon R_1+\epsilon^2 R_2+\dots.\end{aligned}\right\} \tag{3.1}$$

Upon inserting (3.1) into (2.4) and disregarding the quadratic terms, we find the linear problem

$$\Delta_2(\nabla^2\Phi_1+\theta_1) = 0, \tag{3.2a}$$

$$\nabla^2\theta_1 - R_0\Delta_2\Phi_1 = 0. \tag{3.2b}$$

The general solution of (3.2) with the boundary conditions

$$\Phi_1 = \left(\frac{\partial}{\partial z}-\alpha\gamma_{\mathrm{b}}\right)\theta_1 = 0 \quad \text{at} \quad z=-\tfrac{1}{2}, \tag{3.3a}$$

$$\Phi_1 = \left(\frac{\partial}{\partial z}+\alpha\gamma_{\mathrm{t}}\right)\theta_1 = 0 \quad \text{at} \quad z=\tfrac{1}{2} \tag{3.3b}$$

(see appendix A for the derivation of the thermal boundary conditions) can be written as

$$\begin{pmatrix}\theta_1\\ \Phi_1\end{pmatrix} = \begin{pmatrix}g(z)\\ f(z)\end{pmatrix} w(x,y). \tag{3.4}$$

(We have introduced in (3.3) the horizontal wavenumber α of the linear planform function $w(x,y)$.) The function w actually has the representation

$$w(x,y) = \sum_{n=-N}^{N} c_m w_n \equiv \sum_{n=-N}^{N} c_n \exp(i\mathbf{K}_n\cdot\mathbf{r}), \tag{3.5}$$

and satisfies the relation

$$\Delta_2 w = -\alpha^2 w, \quad \langle ww\rangle = 1. \tag{3.6}$$

Here an angle bracket indicates an average over the fluid layer, $\mathbf{r}$ is the position vector, and the horizontal wavenumber vectors $\mathbf{K}_n$ satisfy the properties

$$\mathbf{K}_n\cdot\mathbf{z} = 0, \quad |\mathbf{K}_n| = \alpha, \quad \mathbf{K}_{-n} = -\mathbf{K}_n. \tag{3.7}$$

The coefficients c_n satisfy the conditions

$$\sum_{n=-N}^{N} c_n c_n^* = 1, \quad c_n^* = c_{-n}, \tag{3.8}$$

where the asterisk indicates the complex conjugate. The functions f and g introduced in (3.4) are the unique solutions of the following system of equations:

$$\left.\begin{aligned}(D^2-\alpha^2)f = -g, \quad \langle f^2\rangle = 1, \quad (D^2-\alpha^2)g &= -R_0\alpha^2 f,\\ f = (D-\alpha\gamma_{\mathrm{b}})g = 0 \quad \text{at} \quad z &= -\tfrac{1}{2},\\ f = (D+\alpha\gamma_{\mathrm{t}})g = 0 \quad \text{at} \quad z &= \tfrac{1}{2},\end{aligned}\right\} \tag{3.9}$$

where $D \equiv d/dz$. The function f is also normalized so that $\langle f^2\rangle = 1$. The system (3.9) represents an eigenvalue problem with eigenvalue R_0, and the lowest value R_c of R_0 can be obtained after minimizing R_0 with respect to α (for given γ_{b} and γ_{t}).

In the order ϵ^2, (2.2), (2.4) and (2.5) become

$$\Delta_2(\nabla^2\Phi_2+\theta_2) = 0, \tag{3.10a}$$

$$\nabla^2\theta_2 - R_0\Delta_2\Phi_2 - R_1\Delta_2\Phi_1 = \boldsymbol{\delta}\Phi_1 . \nabla\theta_1, \tag{3.10b}$$

$$\Phi_2 = \bar{\theta}_2 = \frac{\partial\theta_2}{\partial z} - \gamma_b\theta_{2s} = 0 \quad \text{at} \quad z = -\tfrac{1}{2}, \tag{3.10c}$$

$$\Phi_2 = \bar{\theta}_2 = \frac{\partial\theta_2}{\partial z} + \gamma_t\theta_{2s} = 0 \quad \text{at} \quad z = \tfrac{1}{2}, \tag{3.10d}$$

where the bar indicates the horizontal average and θ_{2s} is defined in appendix A. See also this appendix for the derivation of the thermal boundary conditions given by (3.10c), (3.10d).

The solvability conditions for the equations of higher order in ϵ require us to define the following special solutions θ_{1n} and Φ_{1n} of the linear system of equations (3.2)–(3.3):

$$\begin{pmatrix}\theta_{1n}\\ \Phi_{1n}\end{pmatrix} = \begin{pmatrix} g(z)\\ f(z)\end{pmatrix} w_n. \tag{3.11}$$

Multiplying (3.10a) by Φ_{1n}, (3.10b) by $-R_0^{-1}\theta_{1n}$, adding and averaging over the whole layer yields $R_1 = 0$ (appendix B). Equations (3.10) then yield

$$\Phi_2 = \sum_{l,p=-N,\, l\neq -p}^{l,p=N} F(z,\hat{\phi}_{lp})\, c_l c_p w_l w_p + G(z), \tag{3.12a}$$

$$D^2G(z)+\theta_2 = -\sum_{l,p=-N,\, l\neq -p}^{l,p=N} [D^2-2\alpha^2(1+\hat{\phi}_{lp})]\, F(z,\hat{\phi}_{lp})\, c_l c_p w_l w_p, \tag{3.12b}$$

where $$\hat{\phi}_{lp} = \alpha^{-2}(\mathbf{K}_l . \mathbf{K}_p),$$

F is a function of z and $\hat{\phi}_{lp}$, and G is a function of z only. These two functions satisfy the following equations and boundary conditions:

$$\left.\begin{aligned}
&[(D^2-\alpha_s^2)^2 - R_0\alpha_s^2]\, F = \alpha^2(gDf\hat{\phi}_{lp} - fDg),\\
&D^4G = -\alpha^2 D(fg),\\
&G = D^2G = 0 \quad \text{at} \quad z = \pm\tfrac{1}{2},\\
&\left(\frac{\partial}{\partial z} - \alpha_s\gamma_b\right)F = \left(\frac{\partial}{\partial z} + \alpha_s\gamma_t\right)F = 0 \quad \text{at} \quad z = \pm\tfrac{1}{2},\\
&\text{where} \quad \alpha_s = \alpha[2(1+\hat{\phi}_{lp})]^{\frac{1}{2}}.
\end{aligned}\right\} \tag{3.13}$$

In the order ϵ^3, (2.2) become

$$\Delta_2(\nabla^2\Phi_3+\theta_3) = 0, \tag{3.14a}$$

$$\nabla^2\theta_3 - R_0\Delta_2\Phi_3 - R_2\Delta_2\Phi_1 = \boldsymbol{\delta}\Phi_1 . \nabla\theta_2 + \boldsymbol{\delta}\Phi_2 . \nabla\theta_1. \tag{3.14b}$$

Multiplying (3.14a) by Φ_{1n}^*, (3.14b) by $-R_0^{-1}\theta_{1n}^*$, adding and averaging over the whole layer yields

$$-R_2\langle\theta_{1n}^*\Delta_2\Phi_1\rangle = \langle\theta_{1n}^*(\boldsymbol{\delta}\Phi_1 . \nabla\theta_2)\rangle + \langle\theta_{1n}^*(\boldsymbol{\delta}\Phi_2 . \nabla\theta_1)\rangle. \tag{3.15}$$

The average product $\langle\theta_{1n}^*(\boldsymbol{\delta}\Phi_2 . \nabla\theta_1)\rangle$ has no contribution in (3.15) since it vanishes (see appendix B). Equation (3.15) can be simplified to the form

$$R_2F_0c_n = \sum_{l\neq -p} [-(\hat{\phi}_{ml}+\hat{\phi}_{mp})F_1 + F_2]\, c_m c_l c_p \langle w_n^* w_m w_l w_p\rangle + G_2 c_n$$
$$(n = -N, \ldots, -1, 1, \ldots, N), \tag{3.16}$$

where F_1 and F_2 are functions of $\hat{\Phi}_{lp}$ and are given by

$$F_1 = -\alpha^2 \langle gDf[D^2-\alpha_s^2]F\rangle, \tag{3.17a}$$

$$F_2 = -\alpha^2 \langle fg[D^2-\alpha_s^2]DF\rangle, \tag{3.17b}$$

$$G_1 = -\alpha^2 \langle fgD^3G\rangle, \quad F_0 = \alpha^2 \langle fg\rangle. \tag{3.17c}$$

The integral expression $\langle w_n^* w_m w_l w_p\rangle$ in (3.16) differs from zero only if

$$-\mathbf{K}_n+\mathbf{K}_m+\mathbf{K}_l+\mathbf{K}_p = 0. \tag{3.18}$$

This condition yields a much-simplified set of equations

$$R_2 F_0 c_n = \sum_{m=-N}^{N} T_{nm} c_n c_m c_m^* \quad (n=-N,\dots,-1,1,\dots,N), \tag{3.19}$$

where

$$T_{nm} = \begin{cases} \tfrac{1}{2}L(1)+G_1 & (m=\pm n), \\ 2L(\hat{\phi}_{mn})+G_1 & \text{(otherwise)}. \end{cases} \tag{3.20}$$

The function $L(\hat{\Phi}_{lp})$ introduced in (3.20) is defined as

$$L(\hat{\phi}_{lp}) = (1+\hat{\phi}_{lp})F_1(\hat{\phi}_{lp})+F_2(\hat{\phi}_{lp}). \tag{3.21}$$

The solutions of (3.19) and (3.8) are given below in the so-called 'regular' case, in which all angles between two neighbouring $\mathbf{K}$-vectors are equal:

$$|c_1|^2 = \dots = |c_N|^2 = \frac{1}{2N}, \quad R_2F_0 = \frac{1}{2N}\sum_{m=1}^{N}(T_{1m}+T_{1,-m}). \tag{3.22}$$

Using the approximate relationship

$$H_c = \langle w\theta\rangle \approx \epsilon^2\alpha^2\langle fg\rangle \approx \alpha^2(R-R_0)R_2^{-1}\langle fg\rangle \tag{3.23}$$

for the heat transported by convection, we find from (3.20), (3.22) and (3.23): in the case of two-dimensional solution in the form of rolls

$$N=1, \quad H_r \equiv H_c^{\text{rolls}}(R-R_c)^{-1} = 2F_0^2[L(1)+2G_1]^{-1}; \tag{3.24a}$$

in the case of square-pattern convection

$$N=2, \quad \hat{\phi}_{12}=0, \quad H_s = H_c^{\text{squares}}(R-R_c)^{-1} = 4F_0^2[L(1)+4L(0)+4G_1]^{-1}; \tag{3.24b}$$

and in the case of hexagonal cells

$$N=3, \quad \hat{\phi}_{12}=\hat{\phi}_{23}=\hat{\phi}_{31}=\tfrac{1}{2},$$
$$H_h^{\text{hexagons}} = H_c(R-R_c)^{-1} = 6F_0^2[L(1)+6G_1+4L(\tfrac{1}{2})+4L(-\tfrac{1}{2})]^{-1}. \tag{3.24c}$$

4. Stability analysis

The analysis of the nonlinear steady-convection equations has shown that many solutions could exist through the solvability conditions (3.19) even though this manifold represents only an infinitesimal fraction of the manifold of the solutions (3.4) of the linear problem. To distinguish the physically realizable solution among all possible steady solutions, the stability of Φ, θ with respect to arbitrary three-dimensional disturbances $\tilde{\Phi}, \tilde{\theta}$ must be investigated. The equations for the time-dependent disturbances with addition of a time dependence of the form $\exp(\sigma t)$ are given by

$$\Delta_2(\nabla^2\tilde{\Phi}+\tilde{\theta}) = 0, \tag{4.1a}$$

$$-\sigma\tilde{\theta}+\nabla^2\tilde{\theta}-R\Delta_2\tilde{\Phi} = \boldsymbol{\delta}\tilde{\Phi}\,.\,\nabla\theta+\boldsymbol{\delta}\Phi\,.\,\nabla\tilde{\theta}. \tag{4.1b}$$

When the expansions (3.1) is used in (4.1) it becomes evident that the stability equations can be solved by an analogous expansion

$$\begin{pmatrix}\tilde{\Phi}\\ \tilde{\theta}\\ \sigma\end{pmatrix} = \begin{pmatrix}\tilde{\Phi}_1\\ \tilde{\theta}_1\\ \sigma_0\end{pmatrix} + \epsilon \begin{pmatrix}\tilde{\Phi}_2\\ \tilde{\theta}_2\\ \sigma_1\end{pmatrix} + \dots. \tag{4.2}$$

We also restrict ourselves to those disturbances for which R_0 is minimized with respect to α. Then the most-critical disturbances are characterized by $\sigma_0 = 0$. Using the representation

$$\tilde{w}(x,y) = \sum_{n=-\infty}^{\infty} \tilde{c}_n w_n \tag{4.3}$$

for the horizontal dependence of the general three-dimensional disturbance, we consider (4.1) in orders ϵ^n $(n \geqslant 1)$. The possibility of a non-vanishing positive coefficient σ_n appears first in the order ϵ^2, where (4.1) become

$$\Delta_2(\nabla^2\tilde{\Phi}_3 + \tilde{\theta}_3) = 0, \tag{4.4a}$$

$$-\sigma_2\tilde{\theta}_1 + \nabla^2\tilde{\theta}_3 - R_0\Delta_2\tilde{\Phi}_3 - R_2\Delta_2\tilde{\Phi}_1 = \boldsymbol{\delta}\tilde{\Phi}_1 . \nabla\theta_2 + \boldsymbol{\delta}\Phi_1 . \nabla\tilde{\theta}_2 + \boldsymbol{\delta}\tilde{\Phi}_2 . \nabla\theta_1 + \boldsymbol{\delta}\Phi_2 . \nabla\tilde{\theta}_1. \tag{4.4b}$$

Here the solutions $\tilde{\theta}_1$ and $\tilde{\Phi}_1$ have the same form as the corresponding steady solutions θ_1 and Φ_1, provided that the horizontal dependence of the steady solutions is replaced by the expression (4.3). The solutions $\tilde{\Phi}_2$ and $\tilde{\theta}_2$, however, have the form

$$\tilde{\Phi}_2 = \sum_{\substack{l=-\infty,\, p=-N\\ l\neq -p}}^{l=\infty,\, p=N} 2F(z,\hat{\phi}_{lp})\,\tilde{c}_l c_p w_l w_p + G(z)\sum_{m=-N}^{N} 2\tilde{c}_m c_m^*, \tag{4.5a}$$

$$\tilde{\theta}_2 = -\sum_{l=-\infty,\, p=-N,\, l\neq -p}^{l=\infty,\, p=N} 2(D^2-\alpha_s^2)\,F(z,\hat{\phi}_{lp})\tilde{c}_l c_p w_l w_p - D^2G(z)\sum_{m=-N}^{N} 2\tilde{c}_m c_m^*. \tag{4.5b}$$

Multiplying (4.4a) by Φ_{1n}^*, (4.4b) by $-R_0^{-1}\theta_{1n}^*$, adding and averaging over the whole layer yields the following set of equations:

$$\begin{aligned}-\sigma_2\langle g^2\rangle\tilde{c}_n + R_2F_0\tilde{c}_n &= G_1\left[\tilde{c}_n + c_n\sum_{l=-N}^{N}(c_l\tilde{c}_l^* + c_l^*\tilde{c}_l)\right] + \sum_{l\neq -p}[-(\hat{\phi}_{ml}+\hat{\phi}_{mp})F_1 + F_2]\\ &\quad\times(c_m c_l\tilde{c}_p + c_m\tilde{c}_l c_p + \tilde{c}_m c_l c_p)\langle w_n^* w_m w_l w_p\rangle. \end{aligned}\tag{4.6}$$

Using (3.18)–(3.19) in (4.6) yields

$$\sigma_2\langle g^2\rangle\tilde{c}_n + c_n\sum_{m=-N}^{N}\tilde{T}_{nm}c_m^*\tilde{c}_m = 0, \tag{4.7a}$$

where
$$\tilde{T}_{nm} = T_{nm} + T_{n,-m}. \tag{4.7b}$$

Using (3.20) in (4.7b), we find that the matrix $\tilde{T}_{nm}$ has the symmetries

$$\tilde{T}_{nm} = \tilde{T}_{mn} = \tilde{T}_{n,-m} = \tilde{T}_{-n,m}, \tag{4.8a}$$

$$T_{nn} = T_{11} \quad (n = -N,\dots,-1,1,\dots,N). \tag{4.8b}$$

Using (4.8) and following either Schluter *et al.* (1965) or BR, it follows that N eigenvalues σ_2 are zero and the rest of the eigenvalues are real and satisfy the characteristic equation

$$\det|\sigma_2\langle g^2\rangle\delta_{nm} + \tilde{T}_{nm}c_m^*c_n| = 0 \quad (n,m = 1,\dots,N). \tag{4.9}$$

This equation is a polynomial equation in σ_2 of degree N of the form

$$\sum_{n=0}^{N} a_n \sigma_2^n = 0, \tag{4.10}$$

where

$$\left.\begin{aligned} a_N &= (\langle g^2\rangle)^N, \\ a_{N-1} &= \sum_{n=1}^{N} \tilde{T}_{nn}|c_n|^2, \\ a_{N-2} &= \sum_{\substack{n,m=1\\ m>n}}^{N} (\tilde{T}_{nn}\tilde{T}_{mm} - \tilde{T}_{nm}\tilde{T}_{mn})\,|c_n|^2\,|c_m|^2. \end{aligned}\right\} \tag{4.11}$$

The coefficient a_N is clearly positive. Using (3.8), (3.20), (3.22) and (4.7b) we find that

$$a_{N-1} = T_{11} = F_0 R_2^{\text{rolls}}. \tag{4.12}$$

Using (3.17c), (3.23) and the fact that H_c is positive, it follows that F_0 is positive. It is also expected that R_2^{rolls} is positive (as the results in §5 indicate). Hence a_{N-1} is positive. Since all the roots of (4.10) are real and the coefficients a_N and a_{N-1} are both positive, we conclude from the sign rule of Descartes for polynomials that at least one root of (4.10) is positive, provided that the coefficient a_{N-2} is negative. Hence a steady solution ($N > 1$) is unstable if

$$a_{N-2} < 0. \tag{4.13}$$

Equation (4.13) clearly holds if

$$\tilde{T}_{nm} > \tilde{T}_{nn} > 0 \quad (m > n). \tag{4.14}$$

For $N = 1$ the two-dimensional flow in the form of rolls, (4.9), yields

$$\sigma_2^{\text{rolls}}\langle g^2\rangle = -F_0 R_2^{\text{rolls}}. \tag{4.15}$$

Hence $\sigma_2^{\text{rolls}} < 0$ and rolls are stable.

For three-dimensional flow in the form of squares ($N = 2$), (4.9) implies that squares are stable only if the condition (4.13) does not hold.

So far the analysis has been restricted to disturbances that coincide with the basic vectors of the steady motion. We now consider the stability of the steady motion with respect to disturbances in the form of rolls that are not coincident with the basic vector of the steady motion. We define $\mathbf{K}_r$ to be the wavenumber vector of such disturbances. The horizontal dependence of disturbances can be written as

$$\tilde{w}(x, y) = \sum_{r=-1}^{1} \tilde{c}_r \tilde{w}_r, \tag{4.16a}$$

where

$$\tilde{w}_r = \exp(i\tilde{\mathbf{K}}_r \cdot \mathbf{r}). \tag{4.16b}$$

Multiplying (4.4a) by $f\tilde{w}_r^*$, (4.4b) by $-R_0^{\frac{1}{2}} g\tilde{w}_r^*$, adding and averaging over the layer yields the following set of equations:

$$-\tfrac{1}{2}\sigma_2\langle g^2\rangle\,\tilde{c}_r + R_2 F_0 \tilde{c}_r = G_1\tilde{c}_r + \sum_{l \neq -p} [-(\hat{\phi}_{ml} + \hat{\phi}_{mp})\,F_1 + F_2]\,[c_m \tilde{c}_l c_p \langle \tilde{w}_r^* w_m \tilde{w}_l w_p\rangle + c_m c_l \tilde{c}_p \langle \tilde{w}_r^* w_m w_l \tilde{w}_p\rangle]. \tag{4.17}$$

For the steady regular solutions, (4.17) simplifies to

$$-\tfrac{1}{2}\sigma_2\langle g^2\rangle + R_2 F_0 = G_1 + \frac{1}{N}\sum_{m=-N}^{N} L(\hat{\phi}_{rm}). \tag{4.18}$$

For the steady two-dimensional solution in the form of rolls, (4.18) yields

$$\sigma_2\langle g^2\rangle = L(1)-2[L(\hat{\phi}_{r1})+L(-\hat{\phi}_{r1})]. \tag{4.19}$$

For the disturbance rolls that are inclined at an angle of 90° to the basic wavevector $\mathbf{K}_1$ of the steady motion ($\hat{\phi}_{r1}=0$), (4.19) yields a positive σ_2 provided that the condition (4.13) does not hold. Therefore steady rolls are clearly unstable if the steady squares are stable or *vice versa*.

For the steady solution in the form of squares, (4.18) yields

$$\left.\begin{aligned} \sigma_2\langle g^2\rangle &= \tfrac{1}{2}L(1)+2L(0)-L(\hat{\phi}_{r1})-L(-\hat{\phi}_{r1})-L(\hat{\phi}_{r2})-L(-\hat{\phi}_{r2}),\\ \text{where}\qquad |\hat{\phi}_{r2}| &= (1-\hat{\phi}^2_{r1})^{\frac{1}{2}}. \end{aligned}\right\} \tag{4.20}$$

5. Steady solutions

5.1. *The case of infinitely conducting boundaries*

In this subsection we specialize the analysis of §§3 and 4 to the case where the boundaries are isothermal. $\gamma_b=\gamma_t=\infty$ and we have the following results:

$$\left.\begin{aligned} f(z) &= 2^{\frac{1}{2}}\cos\pi z,\quad g(z) = (\pi^2+\alpha^2)\,2^{\frac{1}{2}}\cos\pi z,\\ R_0 &= \alpha^{-2}(\pi^2+\alpha^2)^2,\quad R_c = 4\pi^2,\quad \alpha_c=\pi,\\ G(z) &= \tfrac{1}{4}\pi\sin 2\pi z,\\ F(z,\hat{\phi}_{lp}) &= \frac{\pi(1-\hat{\phi}_{lp})\sin 2\pi z}{2[4+2(1+\hat{\phi}_{lp})+(1+\hat{\phi}_{lp})^2]}. \end{aligned}\right\} \tag{5.1}$$

The function $L(\hat{\phi}_{lp})$ defined in (3.21) and the constants G_1 and F_0 become

$$\left.\begin{aligned} L(\hat{\phi}_{lp}) &= \frac{\pi^8(3+\hat{\phi}_{lp})(1-\hat{\phi}_{lp})^2}{4+2(1+\hat{\phi}_{lp})+(1+\hat{\phi}_{lp})^2},\\ G_1 &= 2\pi^8,\quad F_0=2\pi^4. \end{aligned}\right\} \tag{5.2}$$

Using (3.24) and (5.2), we find

$$\left.\begin{aligned} H_c^{\text{rolls}} &= 2(R-4\pi^2),\quad H_c^{\text{squares}} = \tfrac{28}{17}(R-4\pi^2),\\ H_c^{\text{hexagons}} &= \tfrac{1554}{1079}(R-4\pi^2); \end{aligned}\right\} \tag{5.3}$$

clearly rolls exhibit a higher heat transport than either squares or hexagons.

The condition (4.14) becomes

$$4\pi^8+\frac{2\pi^8(3+\hat{\phi}_{mn})(1-\hat{\phi}_{mn})^2}{7+4\hat{\phi}_{mn}+\hat{\phi}^2_{mn}}+\frac{2\pi^8(3-\hat{\phi}_{mn})(1+\hat{\phi}_{mn})^2}{7-4\hat{\phi}_{mn}+\hat{\phi}^2_{mn}} > 4\pi^8 > 0 \quad (m \neq n). \tag{5.4}$$

Equation (5.4) clearly holds since $0\leqslant\hat{\phi}_{mn}<1$. Hence all three-dimensional solutions are unstable and the only stable flow pattern is that of rolls. This result is identical with that obtained by Schluter *et al.* (1965) for the case of an ordinary medium. The rolls are also stable with respect to any disturbance which is inclined at an arbitrary angle to the basic wavevector of the steady motion, since (4.19) gives a negative σ_2 for any $\hat{\phi}_{r1}$ ($0\leqslant|\hat{\phi}_{r1}|<1$).

5.2. *The case of poorly conducting boundaries*

We now consider the other extreme case where the boundaries are poorly conducting. We avoid to consider the case of zero-conducting boundaries since, as was pointed out in BR, it is physically unrealistic.

We shall discuss briefly the finite-amplitude analysis and the main results of the problem for the case where $\gamma_b = \gamma_t = \gamma \ll 1$. The reader is referred to BR for additional details and background regarding the nonlinear convection in a layer with such boundaries.

As in BR, it is found again that the functional dependence of the value α_c on γ that minimizes R is $\gamma^{\frac{1}{3}}$. Thus it is assumed that $\alpha = \eta\gamma^{\frac{1}{3}}$, where η is a constant of order unity. The linear analysis in BR, as well as in the present study, demonstrates that the value η_c is independent of γ. It turns out that the constant $\mu \equiv \gamma^{\frac{2}{3}}$ could be used as an additional perturbation parameter and the solutions Φ_n, θ_n can be obtained in terms of a series in powers of μ:

$$\begin{pmatrix}\Phi_n\\ \theta_n\end{pmatrix} = \begin{pmatrix}\Phi_n^{(0)}\\ \theta_n^{(0)}\end{pmatrix} + \mu\begin{pmatrix}\Phi_n^{(1)}\\ \theta_n^{(1)}\end{pmatrix} + \dots \tag{5.5}$$

and analogous expression for R_n. The analysis can be carried out in direct analogy to that discussed in BR, and we find the following results:

$$\left.\begin{aligned} f(z) &= (\tfrac{1}{8}-\tfrac{1}{2}z^2)+\alpha^2(-\tfrac{1}{60}z^6-\tfrac{1}{48}z^4+\tfrac{53}{960}z^2-\tfrac{47}{2^8 15})+o(\mu^2),\\ g(z) &= 1+\alpha^2(\tfrac{1}{2}z^4-\tfrac{1}{4}z^2+\tfrac{7}{480})+o(\mu^2),\end{aligned}\right\} \tag{5.6a}$$

$$\left.\begin{aligned} R_0 = 12(1+\frac{2\gamma}{\alpha}+\tfrac{2}{21}\alpha^2)+o(\mu^2), \quad R_c &= 12[1+3(\tfrac{2}{21})^{\frac{1}{3}}\gamma^{\frac{2}{3}}]+o(\mu^2),\\ \alpha_c &= (\tfrac{21}{2})^{\frac{1}{3}}\gamma^{\frac{1}{3}},\end{aligned}\right\} \tag{5.6b}$$

$$\left.\begin{aligned} G(z) &= \frac{\alpha^2}{4!}(\tfrac{1}{5}z^5-\tfrac{1}{6}z^3+\tfrac{7}{240}z),\\ F(z,\hat{\phi}_{lp}) &= \frac{\alpha^2}{4!}(-\tfrac{1}{5}z^5+\tfrac{1}{2}z^3-\tfrac{9}{80}z)\,\hat{\phi}_{lp}.\end{aligned}\right\} \tag{5.6c}$$

The function $L(\hat{\phi}_{lp})$ and the constants G_1 and F_0 are given as

$$\left.\begin{aligned} L(\hat{\phi}_{lp}) &= \tfrac{1}{120}\alpha^4\hat{\phi}_{lp}^2,\\ G_1 = \tfrac{1}{720}\alpha^4, &\quad F_0 = \tfrac{1}{12}\alpha^2.\end{aligned}\right\} \tag{5.7}$$

Using (3.24) and (5.7) we find

$$\left.\begin{aligned} H_c^{\text{rolls}} = \tfrac{5}{4}(R-R_c), &\quad H_c^{\text{squares}} = 2(R-R_c),\\ H_c^{\text{hexagons}} &= \tfrac{5}{4}(R-R_c).\end{aligned}\right\} \tag{5.8}$$

Equations (5.8) indicate that squares exhibit a higher heat transport than either rolls or hexagons.

According to (4.15) rolls are stable. For squares conditions (4.13) or (4.14) does not hold which implies that squares are also stable. However, by the result obtained in §4, rolls become unstable with respect to disturbance rolls that are inclined at an angle of 90° to the basic vector of the steady rolls. In fact the growth rate given by (4.19) becomes

$$\sigma_2\langle g^2\rangle = \tfrac{1}{120}\alpha^4(1-4\hat{\phi}_{r1}^2), \tag{5.9}$$

which shows clearly that σ_2 has the largest positive value for $\hat{\phi}_{r1} = 0$. This result gives an indication of the preferred flow pattern, which consists of square cells (superposition of two roll solutions at a right angle). The same arguments and analysis discussed in BR could be carried out here to conclude that squares are the preferred flow pattern for the case discussed above.

5.3. *The case of arbitrary conducting boundaries*

We now consider the general case where the boundaries have arbitrary thermal conductivity. The solutions to (3.9) and (3.13) are

$$\left.\begin{aligned} f(z) &= \sum_{i=1}^{4} d_i \exp(r_i z), \\ g(z) &= \alpha R_0^{\frac{1}{2}} \sum_{i=1}^{4} (-1)^i d_i \exp(r_i z), \\ F(z, \hat{\phi}_{lp}) &= \sum_{i=1}^{4} \{A_i \exp(2r_i z) + B_i \exp[(r_i + r_{i+1}) z + d_{i+4} \exp(r_{i+5} z)\}, \\ G(z) &= \sum_{i=1}^{4} [A_{i+4} \exp(2r_i z) + d_{i+8} z^{4-i}], \\ \text{where} \quad r_1 &= -r_3 = r_5 = (\alpha^2 + \alpha R_0^{\frac{1}{2}})^{\frac{1}{2}}, \quad r_2 = -r_4 = (\alpha^2 - \alpha R_0^{\frac{1}{2}})^{\frac{1}{2}}, \\ r_6 &= -r_8 = (\alpha_s^2 + \alpha_s R_0^{\frac{1}{2}})^{\frac{1}{2}}, \quad r_7 = -r_9 = (\alpha_s^2 - \alpha_s R_0^{\frac{1}{2}})^{\frac{1}{2}}. \end{aligned}\right\} \quad (5.10)$$

The expressions for the coefficients d_i $(i = 1, \ldots, 12)$, A_i $(i = 1, \ldots, 8)$ and B_i $(i = 1, \ldots, 4)$ introduced in (5.10) are lengthy and are not given in this paper. The complete expressions for these as well as the functions $L(\hat{\phi}_{lp})$, G_1 and F_0 are given in an internal report which can be made available to the reader upon request.

When the general solutions $f(z)$ and $g(z)$ given in (5.10) are used in the boundary conditions and the normalization condition for $f(z)$ given in (3.9), they yield the expressions for d_i $(i = 1, \ldots, 4)$ and the following equation for R_0, α, γ_b and γ_t:

$$\begin{aligned} d_1(-r_1 + \alpha\gamma_b) \exp(-\tfrac{1}{2}r_1) + d_2(r_2 - \alpha\gamma_b) \exp(-\tfrac{1}{2}r_2) \\ + d_3(r_1 + \alpha\gamma_b) \exp(\tfrac{1}{2}r_1) - d_4(r_2 + \alpha\gamma_b) \exp(\tfrac{1}{2}r_2) = 0. \quad (5.11) \end{aligned}$$

R_0 is thus a complicated implicit function of α, γ_t and γ_b through the equation (5.11), and numerical computations are required to determine $R_0(\alpha)$ and R_c for given γ_t and γ_b. The computations are based on a method of half-interval and were carried out at the Computing Centre of the University of Illinois. Numerical computations of R_0 for various values of γ_b and γ_t demonstrate that R_0 is symmetric with respect to γ_b and γ_t:

$$R_0(\alpha, \gamma_b, \gamma_t) = R_0(\alpha, \gamma_t, \gamma_b). \quad (5.12)$$

The three most interesting special cases are as follows.

(i) Both boundaries have the same conductivity γ, $\gamma_t = \gamma_b = \gamma$. Neutral curves for values of $\gamma = 0, 1, 4$ and ∞ are shown in figure 1. The results for $\gamma = 0$ and $\gamma = \infty$ are clearly consistent with the expressions for R_0 given in (5.1) and (5.6). In the actual computations for this case and the next two, the value of 10^{10} is chosen for ∞.

(ii) One of the boundaries (say the upper one) is non-conducting, the other has arbitrary conductivity γ, $\gamma_t = 0$, $\gamma_b = \gamma$. Neutral curves for values of $\gamma = 0, 1, 4$, and ∞ are shown in figure 2.

(iii) One of the boundaries (say the upper one) has infinite conductivity, the other has arbitrary conductivity γ, $\gamma_t = \infty$, $\gamma_b = \gamma$. Neutral curves for the same four values

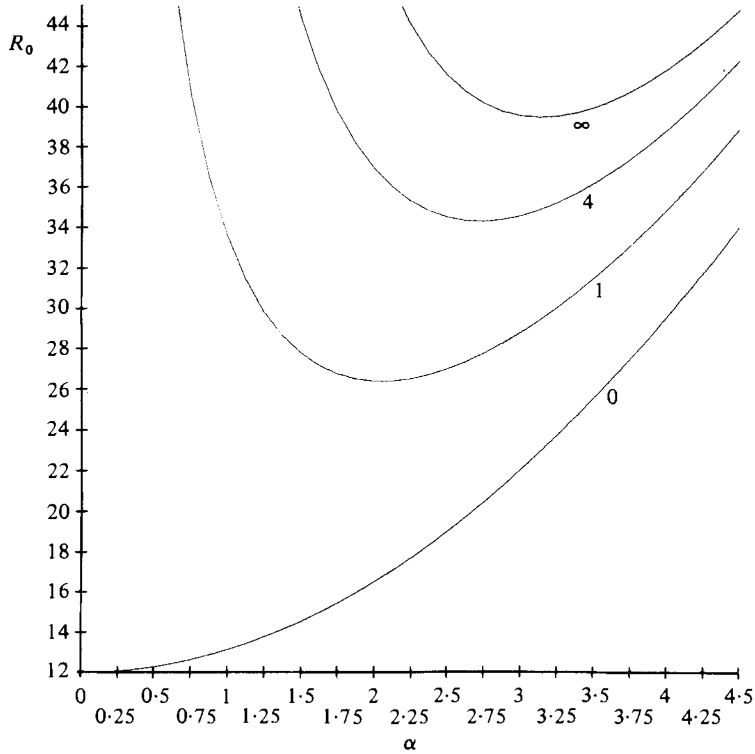

FIGURE 1. Neutral curves for different conductivity ratios γ in the case $\gamma_b = \gamma_t = \gamma$.

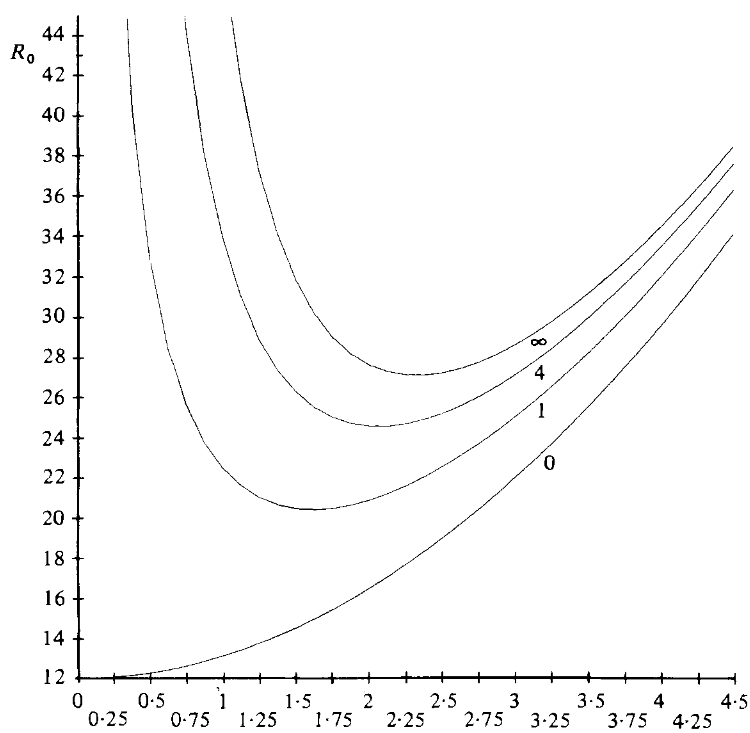

FIGURE 2. Neutral curves for different conductivity ratios γ in the case $\gamma_t = 0$, $\gamma_b = \gamma$.

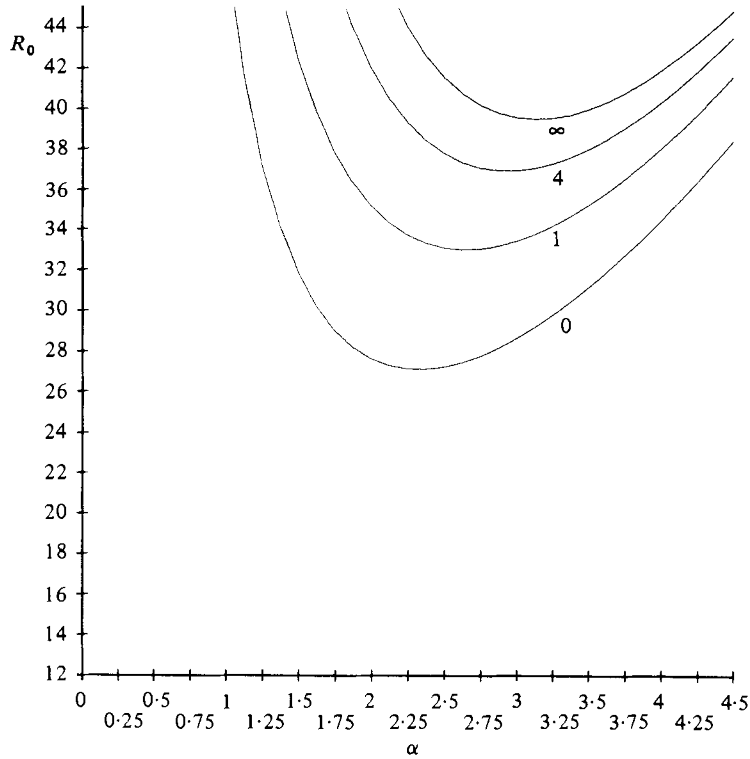

FIGURE 3. Neutral curves for different conductivity ratios γ in the case $\gamma_t = \infty$, $\gamma_b = \gamma$.

of γ as considered in other cases are shown in figure 3. The value of R_0 for a given α in this case is clearly larger than the corresponding one in case (ii). The functional dependence of R_0 with respect to α in case (i) is seen to be approximately intermediate between those in the other two cases.

The minimum value R_c of R_0 with respect to α attained at some $\alpha = \alpha_c$ for given γ_b and γ_t is obviously of importance. Values of R_c and α_c for different values of γ_t and γ_b (for the three cases defined above) are obtained by an additional modified method of half-interval and are presented in table 1. From these results and (5.12) it is seen that R_c increases with either γ_b or γ_t or both. Thus the most-stable situation corresponds to infinite conducting boundaries, and the most-unstable one corresponds to insulating boundaries. R_c is also seen to be most sensitive to γ_b and γ_t in the mid-range of these parameters.

Using (5.10) in (3.17), (3.21) and (3.24), the values of the heat-transfer coefficients H_r, H_s and H_h are computed for the five different cases and are presented in table 2. The main results for each of these cases are as follows.

I. *The case* $\gamma_b = \gamma_t = \gamma$, $0 \leqslant \gamma \leqslant \infty$. Each of the quantities H_r, H_s and H_h increases with γ and reaches its peak at some value of γ in the neighbourhood of $\gamma = 1$ and then decreases with further increase in γ. $H_s = \max(H_r, H_s, H_h)$ for all $\gamma \leqslant \gamma_1 (1 \leqslant \gamma_1 < 4)$. $H_r = \max(H_r, H_s, H_h)$ for all $\gamma > \gamma_1$. $H_h = \min(H_r, H_s, H_h)$ for all the values of γ. The minimum values of H_r, H_s and H_h are attained at the values of γ equal to 0, ∞ and 0 respectively. The quantities H_r, H_s and H_h are most sensitive in the mid-range of γ.

II. *The case* $\gamma_t = \infty$, $\gamma_b = \gamma$, $0 \leqslant \gamma \leqslant \infty$. Each of H_r, H_s and H_h increases with γ

	$\gamma_b = \gamma_t = \gamma$		$\gamma_b = \gamma, \gamma_t = \infty$		$\gamma_b = \gamma, \gamma_t = 0$	
γ	R_c	α_c	R_c	α_c	R_c	α_c
0	12·0	0·00	27·1	2·30	12·0	0·00
0·0001	12·1	0·15	27·1	2·30	12·1	0·15
0·001	12·2	0·20	27·1	2·30	12·1	0·18
0·01	12·8	0·48	27·2	2·31	12·5	0·35
0·1	15·6	0·98	28·1	2·35	14·2	0·78
0·4	20·8	1·55	30·3	2·48	17·3	1·23
0·7	24·1	1·83	31·8	2·55	19·2	1·43
1	26·4	2·03	32·9	2·63	20·4	1·60
4	34·3	2·70	36·9	2·90	24·5	2·05
7	36·3	2·88	37·9	2·98	25·5	2·14
10	37·2	2·95	38·3	3·03	25·9	2·20
100	39·2	3·10	39·3	3·10	26·9	2·28
1000	39·4	3·11	39·4	3·10	27·1	2·30
∞	$4\pi^2$	π	$4\pi^2$	π	27·1	2·30

TABLE 1. Values of R_c and α_c with boundaries of different conductivity

and reaches its peak at some value of γ in the heighbourhood of $\gamma = 1$ and then decreases with further increase in γ. $H_r = \max(H_r, H_s, H_h)$ for all the values of γ. The minimum values of H_r, H_s and H_h are attained at $\gamma = 0$.

III. The case $\gamma_t = 0$, $\gamma_b = \gamma$, $0 \leqslant \gamma \leqslant \infty$. Each of H_r, H_s and H_h seem to increase first with γ and then goes up and down several times as γ increases.

$$H_s = \max(H_r, H_s, H_h) \quad \text{for all } \gamma \leqslant \gamma_2 \quad (0{\cdot}4 \leqslant \gamma_2 < 0{\cdot}7).$$

$H_r = \max(H_r, H_s, H_h)$ for all $\gamma > \gamma_2$. The rate of change of H_r, H_s and H_h with respect to γ is seen to be smaller here than in the first two cases.

IV. *The case* $\gamma_b = \infty$, $\gamma_t = \gamma$, $0 \leqslant \gamma \leqslant \infty$. The qualitative features of H_r, H_s and H_h for this case are similar to the corresponding ones in case II.

V. *The case* $\gamma_b = 0$, $\gamma_t = \gamma$, $0 \leqslant \gamma \leqslant \infty$. The qualitative features of H_r, H_s and H_h for this case are similar to the corresponding ones in case III.

The condition (4.13) has been computed numerically for different integers N and various values of $\hat{\phi}_{mn}$ $(0 \leqslant |\hat{\phi}_{mn}| \leqslant 1)$. In all cases of N and $\hat{\phi}_{mn}$ that have been investigated the condition (4.13) was found to be valid, with the exception of the case $N = 2$, $\hat{\phi}_{mn} = 0$ $(m \neq n)$. This latter case corresponds to squares. Hence all three-dimensional solutions for $N > 2$ are unstable. For squares it was found that (4.13) does not hold for only those values of γ_b and γ_t that yield $H_s > H_r$. Numerical computation of the expression (4.20) for σ_2 at various values of $\hat{\phi}_{r1}$ and $\hat{\phi}_{r2}$ yields a negative σ_2, provided that γ_b and γ_t are chosen such that $H_s > H_r$. Numerical computation of the expression (4.19) for σ_2 at various values of $\hat{\phi}_{r1}$ yields also a negative σ_2, but γ_n and γ_t should now be chosen such that $H_r > H_s$.

The general results obtained in §4 together with the results discussed above conclude that rolls and squares are the only possible stable solutions. Rolls are the only stable solutions in the (γ_b, γ_t)-space for which $H_r \geqslant H_s$. Squares are the only stable solutions in the (γ_b, γ_t)-space for which $H_s \geqslant H_r$.

In order to determine the stability boundary for rolls or squares in the (γ_b, γ_t)-space coordinate system, the equation

$$\tilde{T}_{12} = \tilde{T}_{11} \quad (\text{equivalent to} \quad H_s = H_r) \tag{5.13}$$

	$\gamma_b = \gamma_t = \gamma$			$\gamma_b = \gamma,\ \gamma_t = \infty$			$\gamma_b = \gamma,\ \gamma_t = 0$			$\gamma_b = \infty,\ \gamma_t = \gamma$			$\gamma_b = 0,\ \gamma_t = \gamma$		
γ	H_r	H_s	H_h	H_r	H_s	H_h	H_r	H_s	H_h	H_r	H_s	H_h	H_r	H_s	H_h
0	1·250	2·000	1·250	1·333	0·867	0·929	1·250	2·000	1·250	1·335	0·868	0·930	1·250	2·000	1·250
0·0001	1·258	2·008	1·255	1·333	0·867	0·930	1·258	2·010	1·255	1·335	0·868	0·931	1·258	2·010	1·255
0·001	1·264	2·017	1·259	1·334	0·868	0·936	1·261	2·013	1·260	1·337	0·872	0·933	1·260	2·013	1·257
0·01	1·331	2·100	1·303	1·344	0·872	1·05	1·290	2·032	1·273	1·348	0·876	0·939	1·290	2·033	1·273
0·1	1·650	2·450	1·502	1·508	1·008	1·319	1·407	1·955	1·300	1·503	1·002	1·046	1·406	1·953	1·299
0·4	2·368	2·951	1·876	1·892	1·371	1·453	1·484	1·495	1·325	1·895	1·375	1·321	1·482	1·488	1·200
0·7	2·702	2·966	2·000	2·085	1·574	1·529	1·440	1·189	1·089	2·089	1·581	1·457	1·436	1·180	1·085
1	2·817	2·834	2·014	2·186	1·709	1·546	1·474	1·152	1·084	2·195	1·725	1·536	1·476	1·155	1·086
4	2·430	2·061	1·706	2·177	1·794	1·509	1·408	0·949	0·985	2·176	1·792	1·545	1·406	0·947	0·984
7	2·259	1·886	1·600	2·114	1·744	1·492	1·375	0·906	0·958	2·113	1·742	1·508	1·373	0·905	0·957
10	2·184	1·814	1·554	2·085	1·720	1·446	1·385	0·925	0·967	2·085	1·720	1·492	1·379	0·918	0·963
100	2·023	1·667	1·454	2·010	1·656	1·442	1·326	0·858	0·923	2·010	1·656	1·447	1·317	0·848	0·916
1000	2·004	1·649	1·442	2·004	1·649	1·442	1·335	0·867	0·930	2·004	1·649	1·442	1·336	0·868	0·931
∞	2·000	1·644	1·440	2·000	1·644	1·440	1·335	0·868	0·930	2·000	1·644	1·440	1·333	0·867	0·929

TABLE 2. Values of H_r, H_s and H_h with boundaries of different conductivity

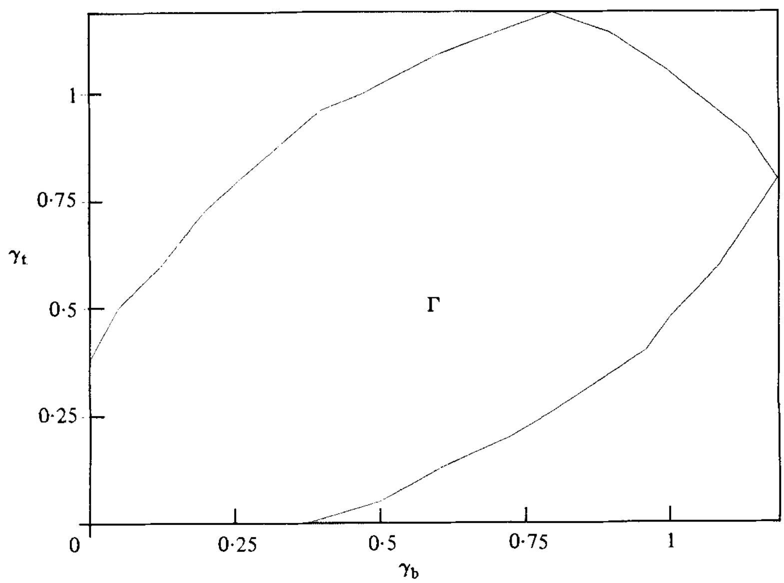

FIGURE 4. Stability boundary for the square cells in the (γ_b, γ_t)-space coordinate system.

is solved numerically. The result is shown in figure 4. Squares are the stable solutions in the region Γ, which includes the origin, while rolls are the stable ones outside Γ. The stability boundary is seen to be symmetric with respect to γ_b and γ_t. The region Γ can be bounded approximately by the lines $\gamma_b = 0$, $\gamma_t = 0$, $\gamma_b + \gamma_t = 2$, and $\gamma_t = \gamma_b \pm 0{\cdot}4$.

6. Discussion

In formulating the present problem we have considered a horizontal layer bounded above and below by infinite half-spaces whose conductivities are constant and, in general, are different from that of the fluid. We used continuity of the temperature and the heat flux at the boundaries to derive the thermal boundary conditions in terms of the two parameters γ_b and γ_t. A different formulation of the thermal boundary conditions in terms of two Biot numbers $B_b = h_b d/\lambda$ and $B_t = h_t d/\lambda$ (h_b and h_t are the heat-transfer coefficients at the lower and upper boundaries respectively) can be done by applying a linear Fourier law for the heat transfer at the boundaries. The temperature boundary conditions then become

$$\left.\begin{aligned} \frac{\partial \theta}{\partial z} &= B_b \theta \quad \text{at} \quad z = -\tfrac{1}{2}, \\ \frac{\partial \theta}{\partial z} &= B_t \theta \quad \text{at} \quad z = \tfrac{1}{2}. \end{aligned}\right\} \tag{6.1}$$

The parameters B_b and B_t can be determined empirically for boundaries with different conductivities, and play the same role as γ_b and γ_t. However, the qualitative features of the problem based on either formulation discussed above is expected to be unchanged.

One of the results obtained in the present study is that $R_c, \alpha_c, H_r, H_s, H_h$ and the vertical component of velocity decrease with decreasing γ_b or γ_t. Hence R_c and α_c are largest for isothermal boundaries, and H_r, H_s, H_h and $\mathbf{u}\,.\,\mathbf{z}$ are smallest for non-conducting boundaries. These conclusions are clearly consistent with one's physical intuition about the problem. As the boundaries become more insulating in nature, given a temperature difference $T_2 - T_1$ across the layer, the perturbation heat flow out of the layer decreases, while the temperature gradient in the interior region away from the boundaries increases. This larger gradient leads to motion at a relatively smaller value of R_c. Since the thermal stabilizing effect decreases, the stabilizing factor of viscosity becomes relatively more significant. Because convection favours the situation where the viscous dissipation is least, the horizontal length of the convection cells increases. Hence α_c decreases and the vertical motion weakens. The associated vertical convective heat transfer in the fluid layer then clearly decreases.

An interesting property of the stable solution discussed in this paper is that the stable solution carries the maximum amount of heat. This result is, however, not surprising, since it has already been proved by Busse (1967) through an extremum principle. Busse's proof is based on the assumption that the amplitude of convection is small, and it does not exclude the possibility that there may be more than one stable solution. This possibility, however, appears to be eliminated in the present problem through the results discussed in the previous sections. In particular, no hysteresis effect is found here.

The uniqueness of the stable solution in the present problem implies that the realized solution is identical with the stable solution that maximizes the heat flux and must clearly be independent of the initial conditions. However, when the effect of the lateral boundaries is significant this result may no longer hold (Straus & Schubert 1979), since the nonlinear effects can be dominated by the sidewall effects in that case.

For each of the five cases described in §5, we have found that there exists a critical value α_c^* in the range $1{\cdot}23 < \alpha_c^* < 2{\cdot}30$ such that for $\alpha_c < \alpha_c^*$ the preferred flow pattern is that of squares. However, for $\alpha_c > \alpha_c^*$, the two-dimensional roll pattern is the preferred solution. The result that *either* a square-cell pattern *or* a two-dimensional-roll pattern (but not both) is the only preferred form of the horizontal structure for given γ_b and γ_t supports the idea that the simplest possible pattern appears to be preferred.

The results of the effects of γ_b and γ_t for the present convection problem in a porous medium are expected also to hold qualitatively in an ordinary medium. Beside the theoretical interest, the results may shed some light on the important and yet unsolved problem of the actual flow pattern of convection and heat transfer in the Earth's upper mantle, where γ_b and γ_t are neither very large nor small. The planform of mantle convection that is needed to generate the observed anomalies does not consist of rolls but is three-dimensional, with rising and sinking jets elongated in the direction of motion (McKenzie *et al.* 1980). The studies by McKenzie and his coworkers suggest that the planform of mantle convection consists of square cells. If this is true, it could lead to some new finding on, for example, the appropriate values of α, γ_b and γ_t. It may then be of interest to extend the present analysis to that for a more realistic model to determine also the quantitative aspect of the results, which could differ from those derived in this paper.

Appendix A

In this appendix we derive the thermal boundary conditions for θ_1 and θ_2. In the spaces $z \leqslant -\frac{1}{2}$ and $z \geqslant \frac{1}{2}$, each of the variables θ_b^e and θ_t^e satisfies the Laplace equation. We now consider the following expansions for θ_b^e, θ_t^e in powers of ϵ:

$$\begin{pmatrix}\theta_b^e\\ \theta_t^e\end{pmatrix} = \sum_{i=1} \epsilon^i \begin{pmatrix}\theta_{bi}^e\\ \theta_{ti}^e\end{pmatrix}. \tag{A 1}$$

In the order ϵ^i, either $\theta^{\mathrm{e}}_{\mathrm{b}i}$ or $\theta^{\mathrm{e}}_{\mathrm{t}i}$ satisfies also the Laplace equation. For $i = 1$ the solutions $\theta^{\mathrm{e}}_{\mathrm{b}1}$ and $\theta^{\mathrm{e}}_{\mathrm{t}1}$ that are bounded at infinity can be written as

$$\left.\begin{aligned} \theta^{\mathrm{e}}_{\mathrm{b}1} &= A^{\mathrm{e}}_1 \exp(\alpha z)\, w(x,y), \\ \theta^{\mathrm{e}}_{\mathrm{t}1} &= B^{\mathrm{e}}_1 \exp(-\alpha z)\, w(x,y), \end{aligned}\right\} \tag{A 2}$$

where A^{e}_1 and B^{e}_1 are constants and $w(x,y)$ is the linear horizontal planform function for the solution θ_1. Using (3.1) and (A 2) in (2.2), we have

$$\left.\begin{aligned} \frac{\partial \theta_1}{\partial z} &= \gamma_{\mathrm{b}} \frac{\partial}{\partial z}\theta^{\mathrm{e}}_{\mathrm{b}1}, \quad \theta_1 = \theta^{\mathrm{e}}_{\mathrm{b}1} \quad \text{at} \quad z = -\tfrac{1}{2}, \\ \frac{\partial \theta_1}{\partial z} &= \gamma_{\mathrm{t}} \frac{\partial}{\partial z}\theta^{\mathrm{e}}_{\mathrm{t}1}, \quad \theta_1 = \theta^{\mathrm{e}}_{\mathrm{t}1} \quad \text{at} \quad z = \tfrac{1}{2}. \end{aligned}\right\} \tag{A 3}$$

Using (A 2), (A 3) we find the boundary conditions (3.3) for the linear solution θ_1. For $i = 2$, the solutions $\theta^{\mathrm{e}}_{\mathrm{b}2}$ and $\theta^{\mathrm{e}}_{\mathrm{t}2}$ that are bounded at infinity can be written as

$$\left.\begin{aligned} \theta^{\mathrm{e}}_{\mathrm{b}2} &= \sum_{l \neq -p} A^{\mathrm{e}}_2 \exp(\alpha z)\, c_l c_p w_l w_p + \bar{\theta}^{\mathrm{e}}_{\mathrm{b}2}, \\ \theta^{\mathrm{e}}_{\mathrm{t}2} &= \sum_{l \neq -p} B^{\mathrm{e}}_2 \exp(-\alpha z)\, c_l c_p w_l w_p + \bar{\theta}^{\mathrm{e}}_{\mathrm{t}2}, \end{aligned}\right\} \tag{A 4}$$

where the bar indicates the horizontal average and A^{e}_2 and B^{e}_2 are two more constants. It should be noted from (A 4) that the horizontal dependence of $\theta^{\mathrm{e}}_{\mathrm{b}2}$ and $\theta^{\mathrm{e}}_{\mathrm{t}2}$ is the same as that of θ_2. Using (3.1) and (A 2) in (2.2) we have

$$\left.\begin{aligned} \frac{\partial}{\partial z}(\theta_2 - \bar{\theta}_2) &= \gamma_{\mathrm{b}} \frac{\partial}{\partial z}(\theta^{\mathrm{e}}_{\mathrm{b}2} - \bar{\theta}^{\mathrm{e}}_{\mathrm{b}2}), \quad \theta_2 - \bar{\theta}_2 = \theta^{\mathrm{e}}_{\mathrm{b}2} - \bar{\theta}^{\mathrm{e}}_{\mathrm{b}2} \quad \text{at} \quad z = -\tfrac{1}{2}, \\ \frac{\partial}{\partial z}(\theta_2 - \bar{\theta}_2) &= \gamma_{\mathrm{t}} \frac{\partial}{\partial z}(\theta^{\mathrm{e}}_{\mathrm{t}2} - \bar{\theta}^{\mathrm{e}}_{\mathrm{t}2}), \quad \theta_2 - \bar{\theta}_2 = \theta^{\mathrm{e}}_{\mathrm{t}2} - \bar{\theta}^{\mathrm{e}}_{\mathrm{t}2} \quad \text{at} \quad z = \tfrac{1}{2}. \end{aligned}\right\} \tag{A 5}$$

Note that $\bar{\theta}_2 = 0$ at $z = \pm\frac{1}{2}$ because the horizontal mean of the boundary temperatures is given as an external parameter of the problem. Using (A 4), (A 5) we find the boundary conditions given in (3.10) for the nonlinear solution θ_2, where $\theta_{2\mathrm{s}}$ introduced in (3.10) has the same form as θ_2, provided that the horizontal dependence of θ_2 is multiplied by $[2(\alpha^2 + \mathbf{K}_l \cdot \mathbf{K}_p)]^{\frac{1}{2}}$.

Appendix B

The expression for R_1 can be written as

$$R_1 = -\langle \theta_{1n} (\boldsymbol{\delta\Phi}_1 \cdot \nabla \theta_1) \rangle \, (\langle \theta_{1n} \Delta_2 \Phi_1 \rangle)^{-1}. \tag{B 1}$$

Multiplying (B 1) by c_n and taking the summation $\sum_{n=-N}^{N}$ yields

$$R_1 = -\langle \theta_1 (\boldsymbol{\delta\Phi}_1 \cdot \nabla \theta_1) \rangle \, (\langle \theta_1 \Delta_2 \Phi_1 \rangle)^{-1}. \tag{B 2}$$

Using the fact that $\langle \theta_1 (\boldsymbol{\delta\Phi}_1 \cdot \nabla \theta_1) \rangle = -\frac{1}{2}\langle \theta_1^2 \nabla \cdot \mathbf{u} \rangle = 0$ and $\langle \theta_1 \Delta_2 \Phi_1 \rangle \neq 0$, we find that $R_1 = 0$.

We will now show that the second average product in the right-hand side of (3.15) vanishes. Using (3.4), (3.11) and (3.12) we have

$$\langle \theta_{1n}^*(\boldsymbol{\delta}\boldsymbol{\Phi}_2 . \nabla\theta_1)\rangle = -\alpha^2 \sum_{l \neq -p} c_m c_l c_p(\hat{\phi}_{ml}+\hat{\phi}_{mp}) \langle g^2DF\rangle \langle w_n^* w_m w_l w_p\rangle$$

$$+\alpha^2 \sum_{l \neq -p} c_m c_l c_p(1+\hat{\phi}_{lp}) \langle D(g^2)\, F\rangle \langle w_n^* w_m w_l w_p\rangle. \quad \text{(B 3)}$$

Since $\langle FD(g^2)\rangle = -\langle g^2DF\rangle$, (B 3) simplifies to

$$\langle \theta_{1n}^*(\boldsymbol{\delta}\boldsymbol{\Phi}_2 . \nabla\theta_1)\rangle = -\alpha^2 \sum_{l \neq -p} c_m c_l c_p(1+\hat{\phi}_{lp}+\hat{\phi}_{ml}+\hat{\phi}_{mp}) \langle g^2DF\rangle \langle w_n^* w_m w_l w_p\rangle. \quad \text{(B 4)}$$

The integral expression $\langle w_n^* w_m w_l w_p\rangle$ in (B 4) is non-zero only if (3.18) holds. However, if (3.18) holds then $1+\hat{\phi}_{lp}+\hat{\phi}_{ml}+\hat{\phi}_{mp} = 0$. Therefore

$$\langle \theta_{1n}^*(\boldsymbol{\delta}\boldsymbol{\Phi}_2 . \nabla\theta_1)\rangle = 0.$$

REFERENCES

BUSSE, F. H. 1967 The stability of finite amplitude cellular convection and its relation to an extremum principle. *J. Fluid Mech.* **30**, 625–649.

BUSSE, F. H. & RIAHI, N. 1980 Nonlinear convection in a layer with nearly insulating boundaries. *J. Fluid Mech.* **96**, 243–256.

JOSEPH, D. D. 1976 *Stability of Fluid Motions* I and II. Springer.

LAPWOOD, E. R. 1948 Convection of a fluid in a porous medium. *Proc. Camb. Phil. Soc.* **44**, 508–521.

MCKENZIE, D., WATTS, A., PARSONS, B. & ROUFOSSE, M. 1980 Planform of mantle convection beneath the Pacific Ocean. *Nature* **288**, 442–446.

PALM, E., WEBER, J. E. & KVERNVOLD, O. 1972 On steady convection in a porous medium. *J. Fluid Mech.* **54**, 153–161.

SCHLUTER, A., LORTZ, D. & BUSSE, F. H. 1965 On the stability of finite amplitude convection. *J. Fluid Mech.* **23**, 129–144.

SCHUBERT, G. & STRAUS, J. M. 1979 Three-dimensional and multicellular steady and unsteady convection in fluid-saturated porous media at high Rayleigh numbers. *J. Fluid Mech.* **94**, 25–38.

STRAUS, J. M. 1974 Large amplitude convection in porous media. *J. Fluid Mech.* **64**, 51–63.

STRAUS, J. M. & SCHUBERT, G. 1978 On the existence of three-dimensional convection in a rectangular box containing fluid-saturated porous material. *J. Fluid Mech.* **87**, 385–394.

STRAUS, J. M. & SCHUBERT, G. 1979 Three-dimensional convection in a cubic box of fluid-saturated porous material. *J. Fluid Mech.* **91**, 155–165.

STRAUS, J. M. & SCHUBERT, G. 1981 Modes of finite-amplitude three-dimensional convection in a rectangular box of fluid-saturated porous material. *J. Fluid Mech.* **103**, 23–32.

ZEBIB, A. & KASSOY, D. R. 1978 Three-dimensional natural convection motion in a confined porous medium. *Phys. Fluids* **21**, 1–3.